Pharmaceutical Sciences and Drug Design
ISSN: 3062-4428
2026, Volume 6, Issue 1, Page No: 19-38

Available online at: www.galaxypub.co/page/journals

Galaxy Publication

Galaxy Publication

Indirubin Targets PI3K–AKT Signaling in Acute Lymphoblastic Leukemia: Integrated Computational and Experimental Evidence

Ravi Kumar[1]*, Neha Sharma[1], Aniket Deshmukh[2], Arjun Nair[1], Meera Pillai[2]

[1]Department of Drug Discovery and Pharmaceutical Sciences, Faculty of Pharmacy, IIT Delhi Health Sciences Unit, New Delhi, India.
[2]Department of Molecular Drug Engineering, Faculty of Pharmaceutical Sciences, IIT Bombay, Mumbai, India.

***E-mail** ✉ ravi.kumar@outlook.com

Received: 04 October 2025; **Revised:** 16 January 2026; **Accepted:** 19 January 2026

ABSTRACT

The present work sought to clarify both the therapeutic activity and the mechanistic basis of indirubin in acute lymphoblastic leukemia (ALL) by integrating network pharmacology approaches with experimental validation. Genes associated with indirubin and ALL were collected from publicly accessible databases to identify potential targets. Protein–protein interaction (PPI) networks were constructed and analyzed in Cytoscape to isolate core genes. Functional enrichment analyses, including Gene Ontology (GO) and Kyoto Encyclopedia of Genes and Genomes (KEGG), were performed to characterize the biological roles and pathways linked to indirubin's activity against ALL. A multi-layered network incorporating drug–disease relationships, functional annotations, and signaling pathways was established. Molecular docking of indirubin with selected core proteins was executed using AutoDock Vina software. To confirm computational predictions, both cell-based in vitro assays and animal-based in vivo experiments were subsequently performed. Analysis of the PPI network identified eight central targets of indirubin in ALL, among which AKT1, CASP3, and the mammalian target of rapamycin were included. GO and KEGG analyses indicated that indirubin may influence ALL progression through diverse biological processes and multiple signaling cascades, with the PI3K–AKT pathway emerging as a key regulatory mechanism. Docking simulations revealed stable, favorable binding interactions between indirubin and the core protein targets. Experimental validation confirmed that indirubin suppressed the proliferation of ALL cells and triggered both cell cycle arrest and apoptosis, with the PI3K–AKT signaling axis likely involved in these effects. By combining network pharmacology, molecular docking, and experimental verification in both in vivo and in vitro models, this study elucidated the biological effects and underlying mechanisms of indirubin in ALL, providing potential directions for future therapeutic development.

Keywords: Indirubin, Acute lymphoblastic leukemia, Network pharmacology, Molecular docking, Experimental validation

How to Cite This Article: Kumar R, Sharma N, Deshmukh A, Nair A, Pillai M. Indirubin Targets PI3K–AKT Signaling in Acute Lymphoblastic Leukemia: Integrated Computational and Experimental Evidence. Pharm Sci Drug Des. 2026;6(1):19-38. https://doi.org/10.51847/Cnpn19Mv34

Introduction

Acute lymphoblastic leukemia (ALL) is a malignant disorder of the blood system characterized by uncontrolled clonal expansion of hematopoietic stem or progenitor cells during their differentiation within the normal hematopoietic hierarchy. The disease is characterized by the excessive accumulation of immature lymphoid cells derived from either the B-cell or T-cell lineages in bone marrow and lymphoid organs [1, 2]. The incidence pattern of ALL follows a bimodal distribution, with higher incidence in early childhood (1–4 years) and again in older adults (≥ 45 years). Epidemiologically, ALL affects approximately one to five individuals per 100,000 annually worldwide, with an estimated 6,660 new cases and 1,560 deaths reported among children and adults combined, according to 2022 data from the United States [3, 4]. Despite substantial improvements in treatment strategies such as multi-drug chemotherapy and hematopoietic stem cell transplantation, which have improved patient

survival, ALL remains difficult to manage due to issues such as drug resistance, minimal residual disease, and disease relapse [5]. Therefore, the development of new therapeutic agents remains an important clinical priority.

Traditional Chinese medicine has been employed in cancer therapy for many years. It is widely valued for its comparatively low toxicity profile, notable pharmacological effects, and reduced tendency to induce drug resistance [6]. In this work, we propose a new therapeutic approach for acute lymphoblastic leukemia (ALL). Indirubin, a key active compound derived from *Indigofera tinctoria* L. and also known under various designations, such as Yuhong Tablet and Couraupitine B, has traditionally been used to treat chronic granulocytic leukemia. Pharmacological research in modern settings has confirmed that indirubin exhibits antiviral, anti-inflammatory, and immune-regulating activities [7, 8]. Over the past several years, increasing evidence has shown that indirubin and its derivatives can suppress tumor cell growth, modulate cell cycle progression, and promote apoptosis across a broad range of human cancers. For example, indirubin has been shown to inhibit ovarian cancer cell proliferation by affecting the STAT3 signaling cascade [9]. In addition, it has been suggested that indirubin may induce ferroptotic cell death in colon cancer therapy [10]. As a bis-indole alkaloid, indirubin has also been reported to interact with tubulin proteins and exert anti-mitotic activity in HeLa cells, particularly when combined synergistically with vinblastine [11]. Despite these findings, studies focusing on the biological effects and mechanistic pathways of indirubin in ALL remain relatively scarce.

In recent years, network pharmacology has developed into an emerging paradigm for drug discovery grounded in contemporary pharmacological science. This approach integrates knowledge and tools from multiple fields, including systems bioinformatics, computational science, and multi-target pharmacology. From the perspective of systems biology, complex diseases such as cancer are not the result of single-gene alterations but rather arise from coordinated disturbances across multiple genes, ultimately disrupting biological network homeostasis. Accordingly, network pharmacology seeks to analyze drug–biological system interactions holistically to restore network balance, identify potential therapeutic targets, enhance therapeutic effectiveness, and reduce adverse reactions, thereby holding significant theoretical and practical value [12, 13]. Molecular docking, on the other hand, is a computational simulation method used to predict the binding orientation and interaction strength between small molecules and protein targets. It is widely used in drug discovery due to its high precision, cost efficiency, and ability to elucidate biochemical mechanisms [14]. Numerous studies have already combined network pharmacology with molecular docking strategies. For instance, the mechanism of resveratrol in diabetic nephropathy has been clarified through an integrated approach involving network pharmacology, molecular docking, and experimental validation [15]. However, only a limited number of studies have applied these strategies to investigate the role of indirubin in ALL.

Therefore, the present research integrates network pharmacology, molecular docking, and experimental validation to systematically investigate the potential targets and molecular mechanisms of indirubin in the treatment of ALL. In addition, preliminary verification was conducted through both cellular and animal experiments. The findings of this study may provide new mechanistic insights and scientific evidence supporting therapeutic development for ALL. The overall workflow of the study is shown in **Figure 1.**

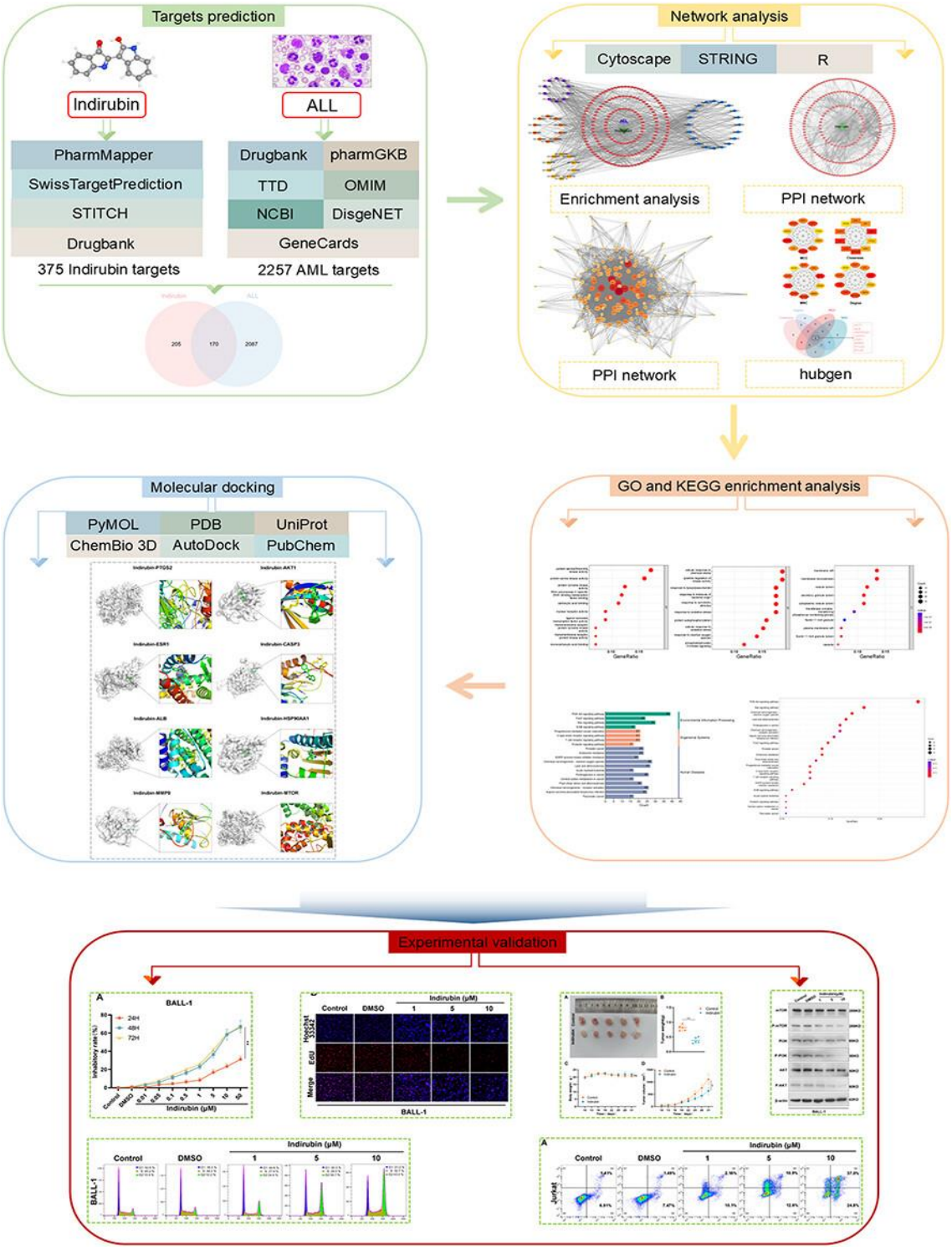

Figure 1. Flowchart of the research process.

Materials and Methods

Drug targets of indirubin

To identify potential molecular targets of indirubin, the PubChem database was first queried using the term "indirubin". The corresponding Structure Data File was downloaded and submitted to the PharmMapper platform for target prediction. In addition, the 2D molecular representation and the Canonical SMILES format of indirubin were obtained from PubChem and used as input to SwissTargetPrediction to infer possible target genes. Further target information was collected from DrugBank and STITCH databases. All retrieved datasets were subsequently combined, and duplicate entries were removed to ensure a non-redundant target pool.

Screening therapeutic targets for all

Genes associated with acute lymphoblastic leukemia (ALL) were retrieved from four independent resources: DisGeNET, GeneCards, the National Center for Biotechnology Information (NCBI), and Online Mendelian Inheritance in Man (OMIM). Each database was searched using the keyword "acute lymphoblastic leukemia". Within GeneCards, only entries with a score exceeding 10 were retained for analysis. After extraction, gene lists from all databases were merged, and redundant records were eliminated to establish a unified ALL-related gene set. Overlapping genes between indirubin-related targets and ALL-associated genes were identified using the SangerBox platform, and a Venn diagram was generated. These shared genes were considered potential therapeutic targets of indirubin in ALL and were selected for subsequent analyses.

Construction of protein–protein interaction (PPI) network and hub gene analysis

To explore functional relationships among candidate targets, a protein–protein interaction (PPI) network was constructed using the STRING database. The shared gene set was uploaded to STRING, with species limited to "Homo sapiens" and a confidence score threshold of 0.4. Isolated nodes were excluded from the network, while default settings were retained for all other parameters. The resulting interaction data were imported into Cytoscape 3.7.2 for visualization and network analysis. Hub genes were further identified using the CytoHubba plugin. Four topology-based algorithms—Degree, Maximum Neighborhood Component (MNC), Maximal Clique Centrality (MCC), and Closeness—were applied independently to rank genes, and the top 10 candidates from each method were extracted. Final hub genes were determined by intersecting these ranked gene sets.

Gene ontology (GO) and kyoto encyclopedia of genes and genomes (KEGG) enrichment analysis

To systematically characterize the biological functions and pathways associated with indirubin in ALL, GO and KEGG enrichment analyses were performed. GO analysis included biological processes, cellular components, and molecular functions, while KEGG analysis identified relevant signaling pathways. Before analysis, intersecting genes were converted to Entrez IDs using Perl 5.3.8. All enrichment analyses were conducted in R 4.3.1 (R Foundation for Statistical Computing, Vienna, Austria) using the following packages: clusterProfiler, org.Hs.eg.db, enrichplot, and ggplot2. A significance threshold of $P < 0.05$ was applied. The top 10 genes were selected for GO enrichment, whereas the top 20 genes were used for KEGG pathway analysis. Pathway visualization was generated using the Bioinformatics online platform (http://www.bioinformatics.com.cn/). Finally, a comprehensive drug–disease–target–function–pathway network was constructed in Cytoscape to depict the multi-level relationships among compounds, disease, targets, functions, and signaling pathways.

Molecular docking

To assess the binding interactions between indirubin and key proteins, molecular docking simulations were conducted. The 2D structure of indirubin was obtained from PubChem and converted to a 3D conformation using Chem3D. The 3D structures of selected core proteins were retrieved from the UniProt and Protein Data Bank (PDB) databases. Before docking, PyMOL software was used to remove water molecules, native ligands, and peptide residues from protein structures. Active binding sites were then predicted using AutoDock Tools 1.5.7. Docking simulations between indirubin and target proteins were performed using AutoDock Vina to determine optimal binding conformations and calculate binding free energies. More negative energy values indicated stronger binding affinity. The resulting docking poses were visualized in PyMOL.

Cell lines and cell culture

The BALL-1 and Jurkat cell lines used throughout the experiments were obtained from the American Tissue Culture Collection (Manassas, Virginia, United States of America). Cells were maintained in RPMI 1640 medium (Gibco) supplemented with 10% fetal bovine serum (Gibco), 100 U/mL streptomycin, and 100 U/mL penicillin (Gibco). Cultivation was performed at 37°C in a humidified incubator under 5% CO_2.

CCK8

Cell viability following treatment with indirubin (MCE, HY-N0117) was determined using the Cell Counting Kit-8 (CCK-8) assay (NCM Biotech). For this assay, ALL cells were seeded into 96-well plates at a density of 1×10^4 cells per well. Treatment groups included indirubin at concentrations of 1, 5, and 10 μM, along with a blank

control (BC) and a solvent control (DMSO). After incubation periods of 24, 48, and 72 hours, 10 μL of CCK-8 reagent was added to each well. Following a 3-hour reaction period, absorbance was measured at 450 nm using a microplate reader (BioTek, Vermont, USA). Cell proliferation was calculated using the following equation: absorbance of (control group – experimental group)/absorbance of (control group – blank group) × 100%. Each condition included five replicate wells (n = 5), and all experiments were independently performed three times (n = 3 independent experiments).

EdU

The proliferative ability of ALL cells after indirubin exposure was evaluated using an EdU incorporation assay kit (Beyotime, C0075S) according to the manufacturer's instructions. Cells were plated in six-well plates at a density of 3×10^5 cells per well, using the same dose groups and experimental setup as in the CCK-8 assay. After 48 hours of treatment, EdU was added at a final concentration of 50 μmol/L and incubated for 2 hours. Cells were then collected by centrifugation and rinsed with phosphate-buffered saline (PBS). Fixation was performed with 4% paraformaldehyde, followed by permeabilization with 0.3% Triton X-100. Nuclear staining was performed using Hoechst 33342 (Beyotime, C0075S). The stained cells were resuspended in PBS, mounted onto slides, and visualized under a fluorescence microscope (Olympus, Japan). Image acquisition and quantitative analysis were performed using ImageJ (National Institutes of Health, Bethesda, MD, USA). Each experiment was repeated independently three times (n=3 independent experiments).

Cell apoptosis assay

Apoptotic cell death was assessed using an Annexin V-FITC/PI staining kit (Beyotime, C1383M). ALL cells were seeded at a density of 3×10^5 cells per well in six-well plates and exposed to indirubin for 48 hours. The same concentration scheme used in the CCK-8 assay was applied. After treatment, cells were harvested, washed twice with PBS, and double-stained with Annexin V and propidium iodide (PI). Samples were incubated for 15 minutes at room temperature in the dark before analysis. Flow cytometry was performed using a BD Biosciences system (San Jose, USA), and data were processed using FlowJo 10 software. Each experimental set was independently repeated three times (n = 3 independent experiments).

Cell cycle assay

To evaluate how indirubin affects cell cycle progression in ALL cells, a Cell Cycle Kit (Beyotime, C1052) was used. Cells were processed under the same experimental conditions described for the apoptosis assay. After 48 hours of treatment, cells were collected by centrifugation, washed with ice-cold PBS, and fixed using pre-cooled 70% ethanol. The fixed cells were then rinsed twice with PBS before being incubated with propidium iodide (PI) staining solution for 30 minutes at room temperature in the dark. Cell cycle distribution was analyzed by flow cytometry (BD Biosciences, San Jose, USA), and data were analyzed using FlowJo 10 software. Each experiment was independently repeated three times (n = 3 independent experiments).

Western blotting

ALL cells exposed to drugs were grouped and treated consistently with prior experimental setups. Following collection, cells were washed with PBS and lysed using RIPA buffer supplemented with protease inhibitors. The lysates were kept on ice and mechanically disrupted by sonication. After centrifugation at 4 °C at 15,000 rpm for 15 minutes, the clarified supernatant was obtained. Protein concentration was quantified using a bicinchoninic acid (BCA) assay kit (Beyotime, P0010) according to the manufacturer's instructions. Proteins were then separated using SDS-PAGE (10% or 12% gels) and transferred onto PVDF membranes (Millipore). Membranes were blocked with 5% skim milk for 1 hour at room temperature, then incubated overnight with primary antibodies at 4 °C. After washing, membranes were incubated with secondary antibodies for 2 hours at room temperature. Protein bands were detected using an enhanced chemiluminescence system. Each experiment was independently performed three times (n = 3 independent experiments).

Extraction of bone marrow mononuclear cells

Bone marrow samples were obtained from six patients with clinically diagnosed ALL (n = 6) for this study. Each specimen was diluted by mixing with an equal volume of saline or PBS. The resulting suspension was carefully layered onto 5 mL of density gradient medium in a 15 mL centrifuge tube to maintain clear phase separation.

Samples were centrifuged at 2000 rpm for 25 minutes at room temperature, forming four layers: plasma, mononuclear cells, separation medium, and erythrocytes (from top to bottom). The mononuclear cell layer was carefully extracted and transferred into a new tube, then resuspended in 10 mL of saline or PBS and centrifuged again at 2000 rpm for 10 minutes. After discarding the supernatant, the washing step was repeated once more. The resulting mononuclear cell pellet was collected for downstream analyses. Ethical approval for the use of ALL patient bone marrow samples was granted by the Ethics Committee of Guizhou Medical University.

Xenograft tumor model

An in vivo evaluation of indirubin was conducted using a xenograft model established in ten female NOD SCID gamma mice aged 6–8 weeks. Each mouse was subcutaneously inoculated on the right flank with 100 µL of serum-free medium containing 1×10^7 BALL-1 cells. After allowing 3 weeks for tumor establishment, animals were randomly assigned to two groups of 5 mice each (n = 5 per group). One group received daily oral gavage of indirubin at 25 mg/kg, while the control group received 0.1% dimethyl sulfoxide under the same regimen for 3 weeks. Tumor growth was monitored at 5-day intervals by measuring tumor volume. At the end of the treatment period, mice were euthanized, and tumors were excised for imaging and weighing. All procedures involving animals were conducted in accordance with ethical standards and approved by the Animal Ethics Committee of Guizhou Medical University.

Statistical analyses

All quantitative data are reported as mean values accompanied by standard deviation (SD). Statistical significance between groups was evaluated using Student's t-test, as well as one-way or two-way analysis of variance (ANOVA), followed by Tukey's post-hoc test for multiple comparisons. GraphPad Prism version 8.0 (San Diego, CA, USA) was used for all statistical computations. A threshold of $P < 0.05$ was set as the criterion for statistical significance.

Results and Discussion

Potential targets of indirubin in ALL and construction of PPI network

Structural information of indirubin in both 2D and 3D formats was obtained from the PubChem database **(Figures 2a and 2b)**. Target prediction for indirubin was performed using the DrugBank, SwissTargetPrediction, PharmMapper, and STITCH databases, yielding 375 unique protein targets after integration and duplicate elimination. In parallel, ALL-associated genes were compiled from the Therapeutic Target Database, PharmGKB, DrugBank, OMIM, NCBI, GeneCards (filtered by relevance score > 10), and DisGeNET, yielding a total of 2,257 disease-related genes. Comparison between indirubin-related targets and ALL-associated genes identified 170 overlapping genes as potential therapeutic targets **(Figure 2c)**.

Interaction networks were then constructed using STRING and visualized in Cytoscape to represent drug–target relationships and shared gene interactions **(Figures 2d and 2e)**. As shown in **Figure 2e**, nodes with larger sizes and darker coloration correspond to higher network connectivity, indicating greater biological importance.

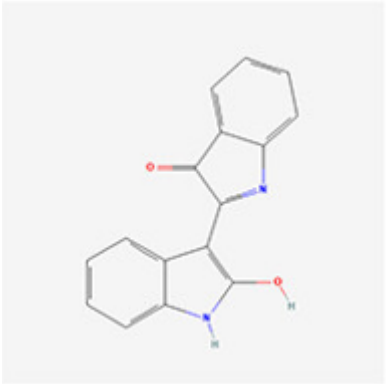

a)

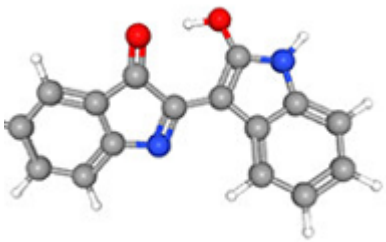

b)

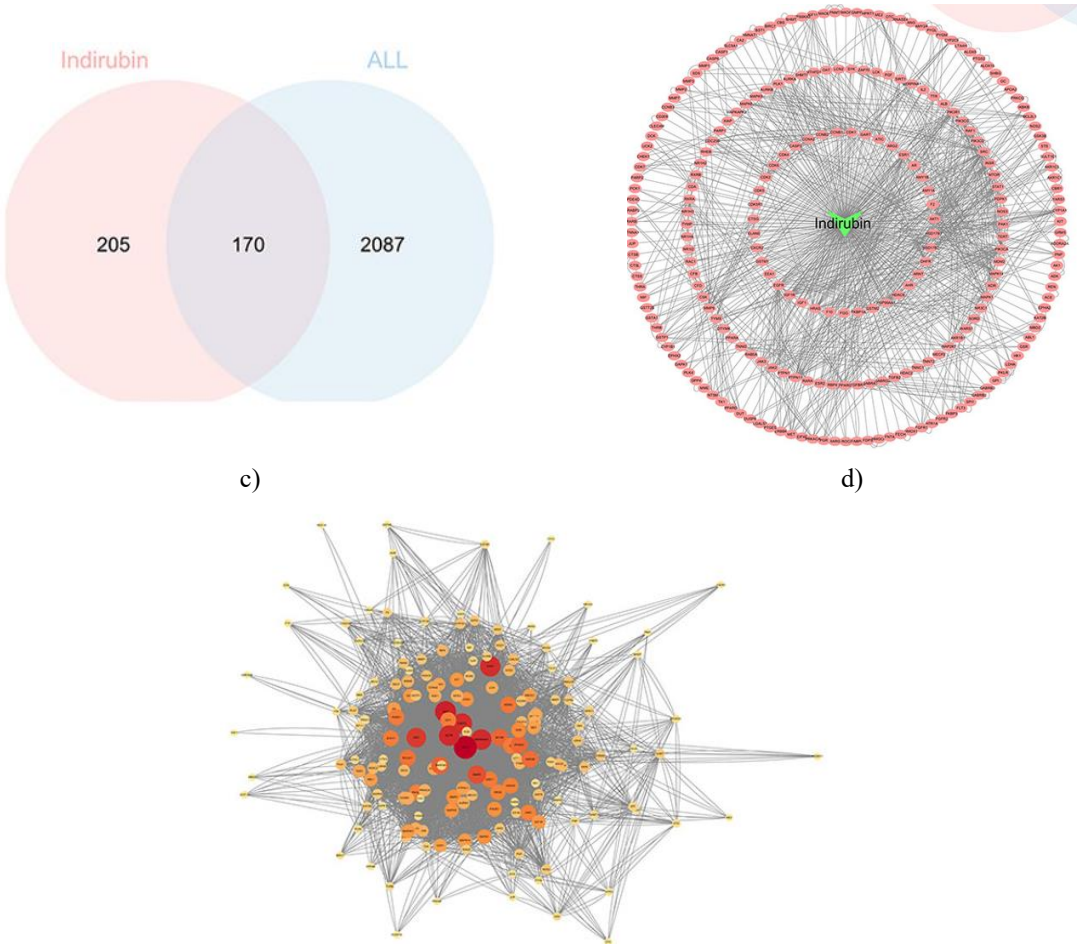

Figure 2. Potential targets of indirubin action in ALL and construction of the PPI network: (a and b) 2D and 3D structures of indirubin, (c) Venn diagram illustrating overlapping genes between indirubin and ALL, (d) PPI network of indirubin-related targets, (e) PPI network of intersecting genes. Node size and color intensity reflect the degree of connectivity.

Enrichment analysis and construction of the integrated network diagram

To further explore functional implications, GO and KEGG enrichment analyses were performed on the 170 intersecting genes using R software. Results were visualized across multiple layers of biological interpretation. For GO analysis, the 10 most significantly enriched terms in each category—biological process (BP), cellular component (CC), and molecular function (MF)—were selected for presentation **(Figure 3a)**. Within BP, key enriched processes included "cellular response to chemical stress", "positive regulation of kinase activity", and "protein autophosphorylation". CC-related terms were mainly associated with "membrane raft", "membrane microdomain", and "vesicle lumen", while MF enrichment highlighted "protein serine/threonine kinase activity", "ligand-activated transcription factor activity", and "transmembrane receptor protein kinase activity".

KEGG pathway analysis identified the top 20 significantly enriched signaling pathways **(Figure 3b)**. The results indicated that indirubin may exert its anti-ALL effects primarily through the PI3K-Akt, FoxO, and Ras signaling pathways. Functional classification of KEGG-related genes is presented in **Figure 3c**, where the majority were grouped under "Human Diseases", particularly within "Hematological and Solid Tumors" and "Organismal Systems", while a smaller portion belonged to "Environmental Information Processing". Based on pathway enrichment, the PI3K-Akt signaling pathway was selected for further detailed analysis. A dedicated PPI network was also constructed for genes in this pathwa, with node size and color depth indicating gene relevance. Finally, an integrated multi-layer network linking drug–disease–functional annotation–signaling pathways was generated **(Figure 3d)**. In this model, purple, orange, and yellow nodes correspond to the top 10 GO terms for BP, CC, and MF, respectively, while blue nodes represent the top 20 KEGG-enriched pathways.

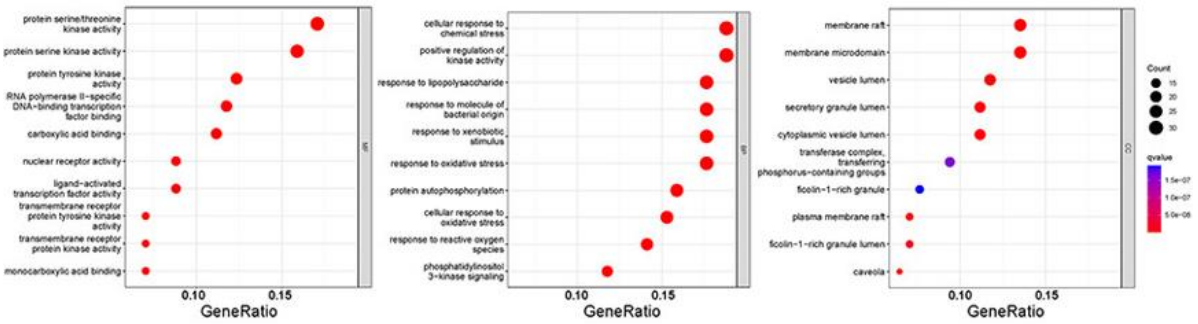

a)

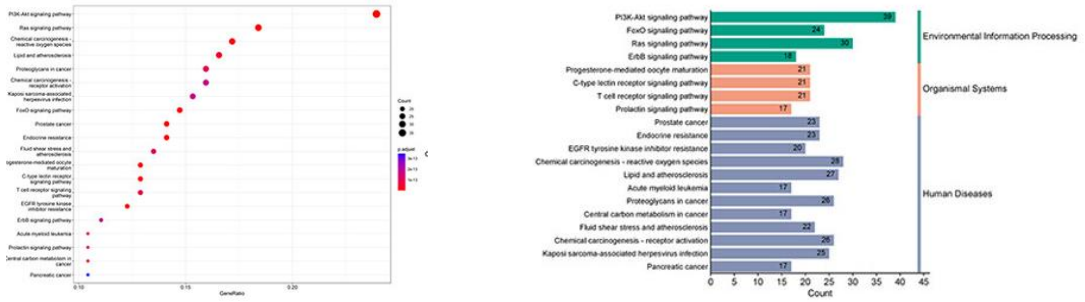

b) c)

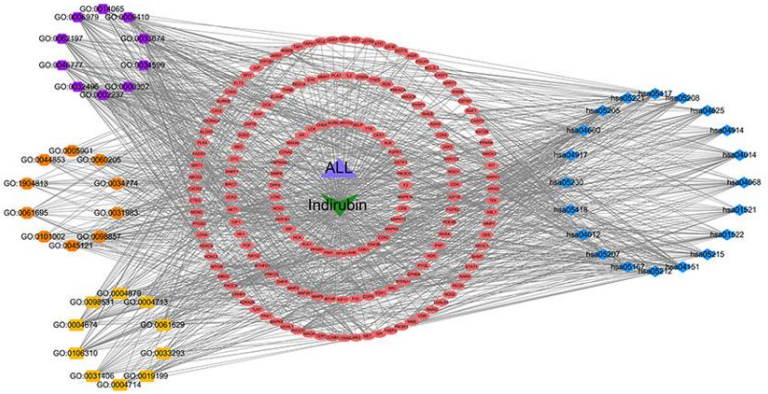

d)

Figure 3. Enrichment analysis and construction of the integrated network diagram: (a) GO enrichment analysis results. Circle size reflects gene count per term, while color intensity represents statistical significance (P-value). (b) KEGG pathway enrichment analysis. The X-axis indicates the number of genes per pathway, and colors denote KEGG categories. (c) GO-based functional classification of key targets. (d) Integrated drug–disease–function–pathway network. The central red node represents core indirubin targets in ALL. Purple, orange, and yellow nodes on the left indicate the top 10 BP, CC, and MF GO terms, respectively, while blue nodes correspond to the top 20 KEGG pathways.

Core gene screening

Hub gene identification was carried out on the 170 intersecting genes using the CytoHubba plugin in Cytoscape. Four network topology algorithms—MCC, MNC, Degree, and Closeness—were applied to prioritize candidate genes. The highest-ranking 10 genes from each algorithm are shown in **Figures 4a–4d**, where node colors transition from light yellow to deep red, representing increasing centrality and biological importance. By integrating results from all four methods, eight overlapping core genes were ultimately obtained **(Figure 4e).**

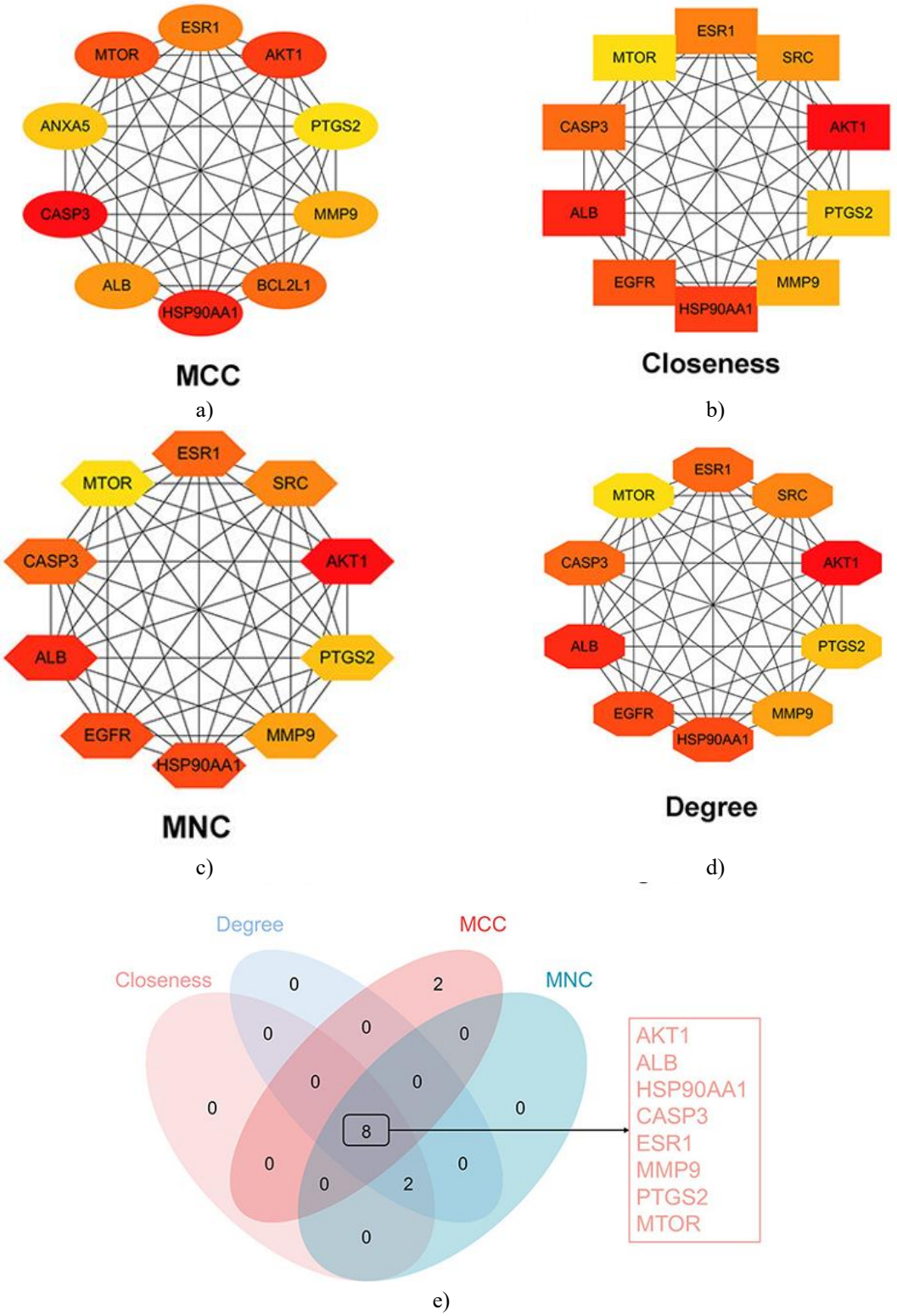

Figure 4. Core gene screening. Top 10 hub genes identified using (a) MCC, (b) Closeness, (c) MNC, and (d) Degree algorithms. (e) Venn diagram illustrating shared core targets among MCC, MNC, Degree, and Closeness.

Molecular docking

To evaluate potential binding interactions between indirubin and key proteins, molecular docking analysis was performed. Three-dimensional structures of the eight core proteins were retrieved from the Protein Data Bank (PDB), and docking simulations were conducted using AutoDock Vina. Binding affinity was assessed based on binding free energy, where more negative values correspond to stronger and more stable ligand–receptor

interactions. Binding energies below −5.0 kcal/mol were considered moderate affinity, whereas values lower than −7.0 kcal/mol indicated strong binding potential. The most stable docking conformations for each target were visualized using PyMOL 2.5 **(Figure 5)**, focusing on the lowest-energy complexes. Overall, indirubin exhibited strong binding across all eight targets, suggesting these proteins may represent key molecular targets. In addition, expression analysis using data from The Cancer Genome Atlas (TCGA) and the Genotype-Tissue Expression (GTEx) database revealed significant dysregulation of these genes in ALL samples ($P < 0.05$).

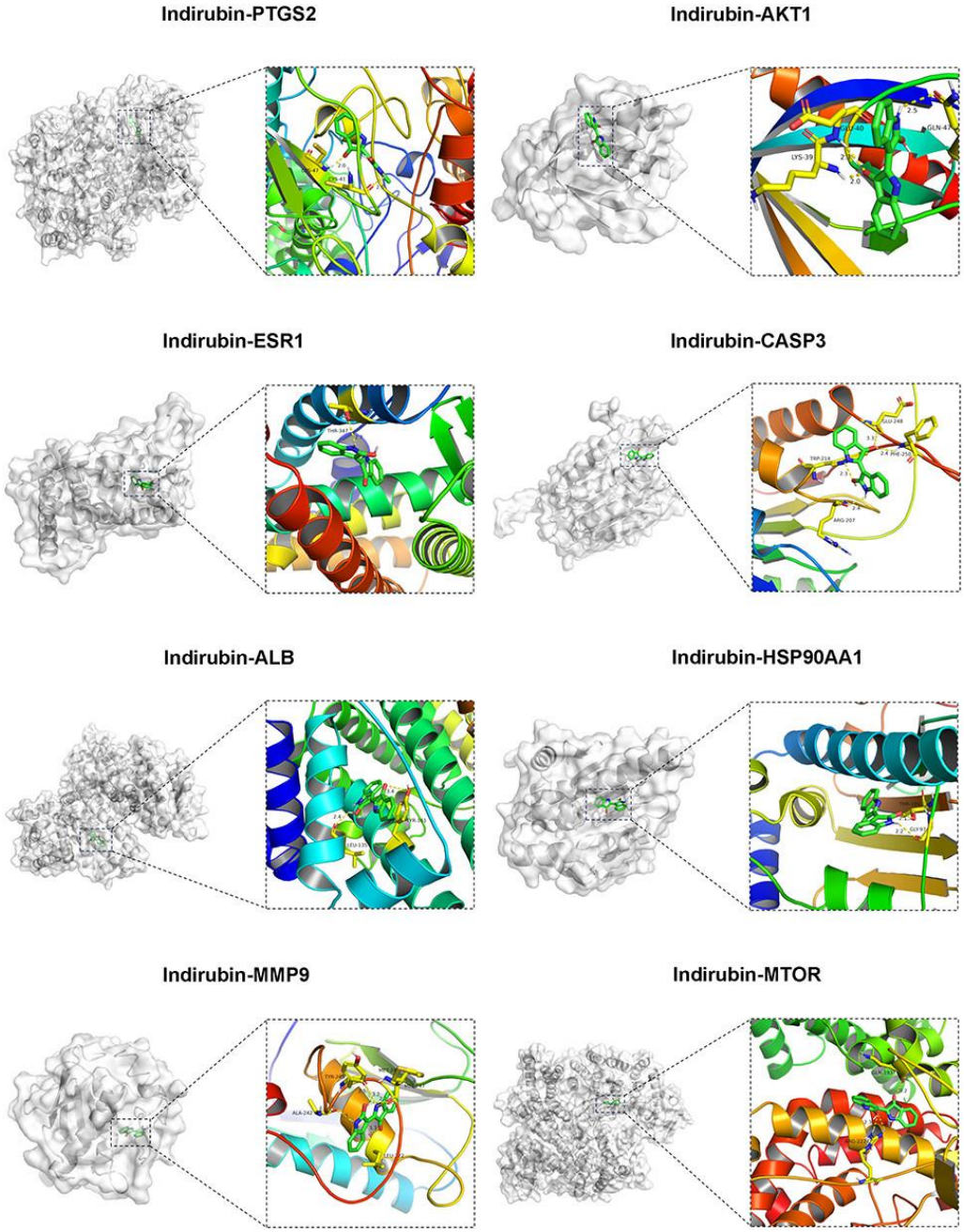

Figure 5. Three-dimensional docking visualization of indirubin with eight core targets showing minimum binding energy conformations.

Indirubin inhibits ALL cell proliferation

The anti-proliferative effect of indirubin on ALL cells was examined using the CCK-8 assay under different concentrations and time points. Results indicated a clear dose-dependent inhibition of cell viability, with higher concentrations producing stronger suppression **(Figures 6a and 6b)**. Time-course analysis showed that inhibitory effects increased up to 48 hours but did not further rise at 72 hours **(Figures 6a and 6b)**. Based on these

observations, subsequent experiments were designed to use 1 μM, 5 μM, and 10 μM indirubin for a 48-hour treatment duration.

The EdU assay further confirmed that DNA synthesis activity in ALL cells progressively decreased as indirubin concentration increased **(Figures 6c and 6d)**. Each experiment was independently repeated three times.

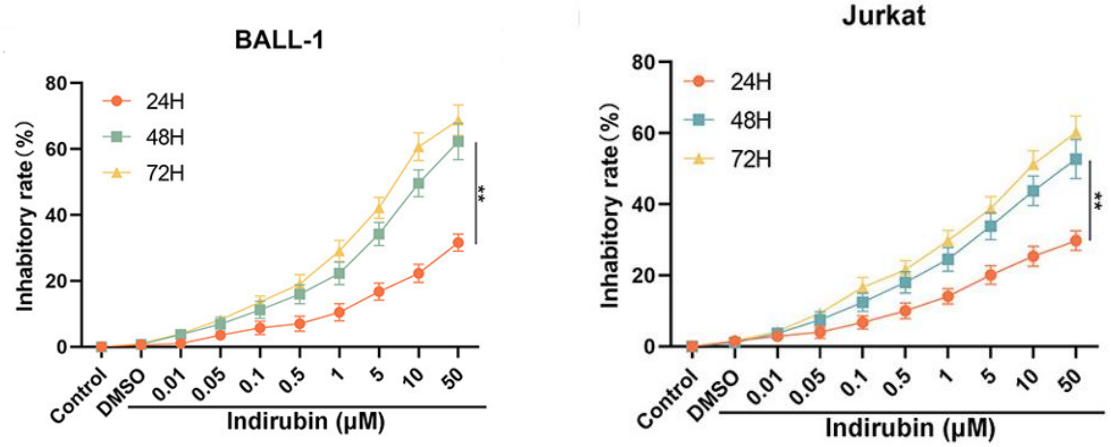

a)

b)

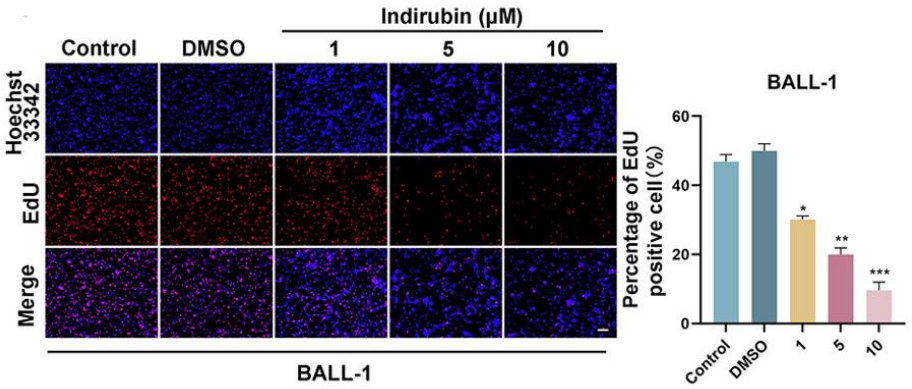

c)

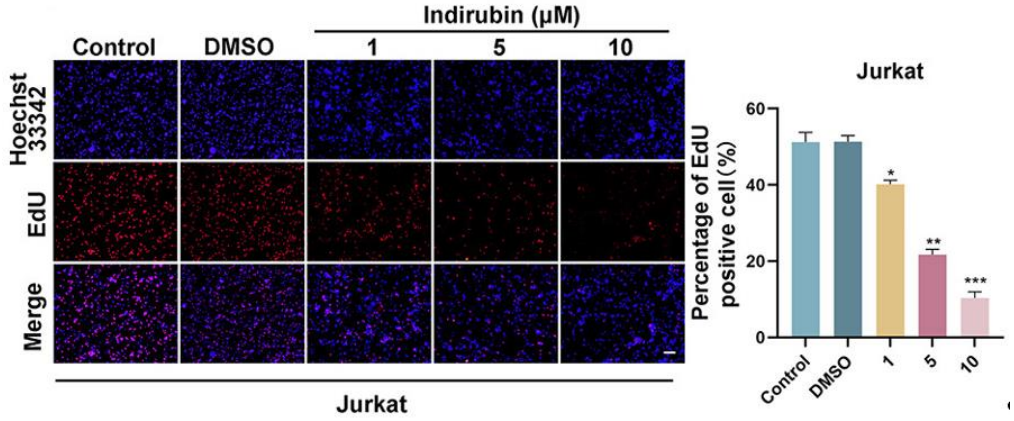

d)

Figure 6. Effect of indirubin on ALL cell proliferation: (a and b) CCK-8 assay showing dose- and time-dependent inhibition of BALL-1 and Jurkat cells after 24, 48, and 72 hours, and (c and d) EdU assay demonstrating reduced proliferative activity in ALL cells. Data are shown as mean ± SD; n = 5. *P < 0.05; **P < 0.01; ***P < 0.001 vs DMSO or control group. Scale bar: 100 μm. Abbreviations: DMSO = dimethyl sulfoxide; SD = standard deviation; CCK-8 = Cell Counting Kit-8.

Indirubin induces apoptosis in ALL cells

Apoptotic changes were evaluated using Annexin V-FITC/PI staining, which showed a marked increase in apoptosis rates in both ALL cell lines following indirubin treatment in a concentration-dependent manner **(Figures 7a and 7b).** Western blot analysis of apoptosis-associated proteins revealed that caspase-3 levels remained largely unchanged, whereas Bax and cleaved caspase-3 were upregulated, and Bcl-2 expression was downregulated **(Figure 7c)**. These results indicate that indirubin promotes apoptosis in ALL cells by modulating the expression of apoptosis-related proteins.

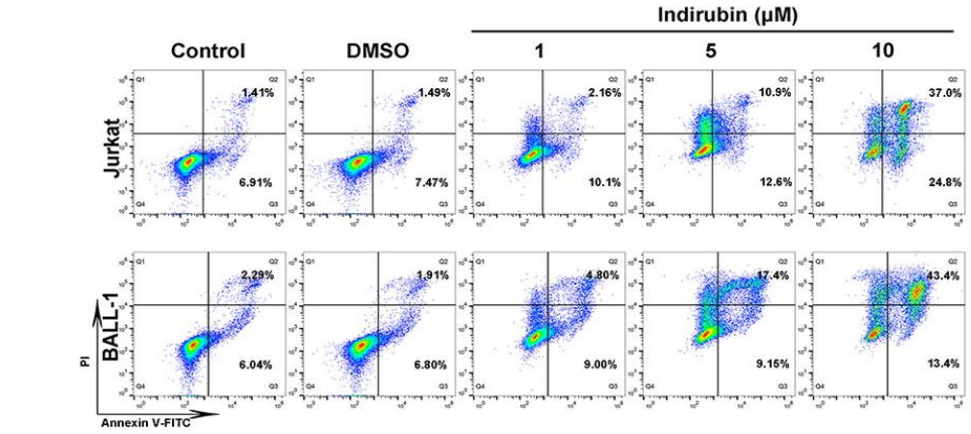

a)

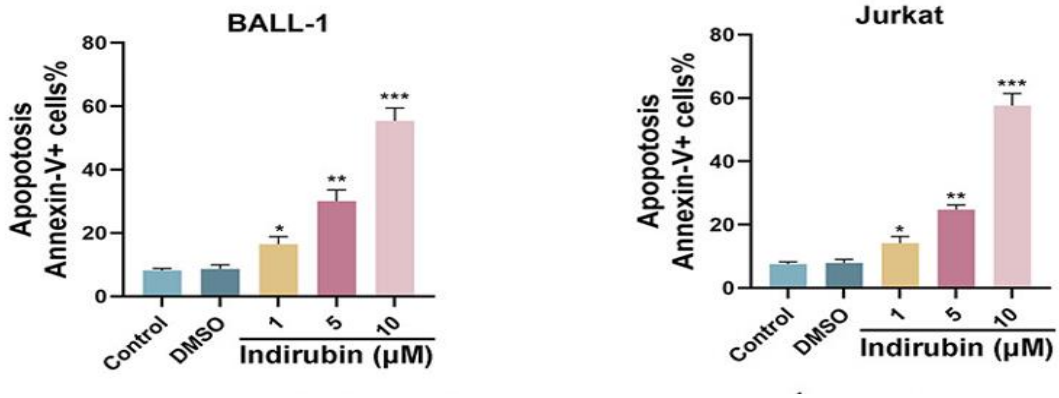

b)

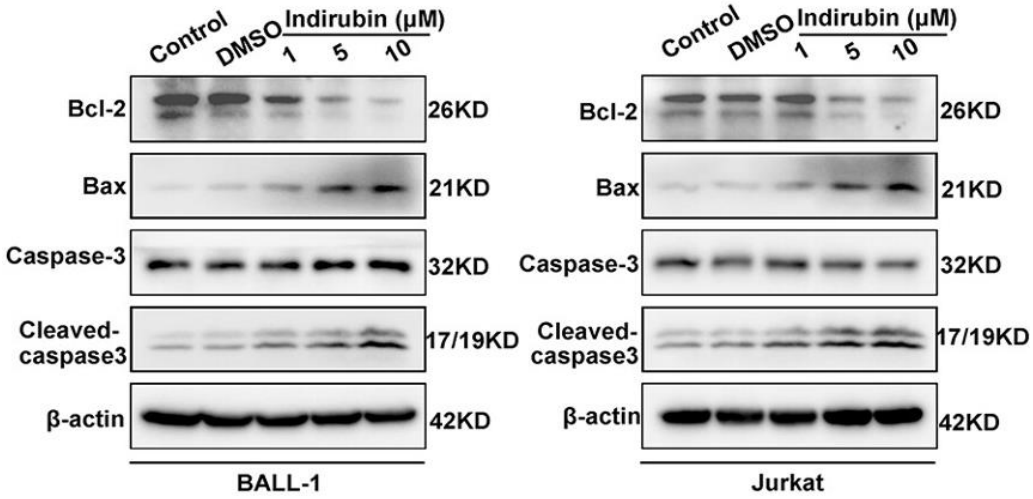

c)

Figure 7. Effect of indirubin on apoptosis in ALL cells: (a and b) Flow cytometric analysis of apoptosis using Annexin V-FITC/PI staining, and (c) Expression of apoptosis-related proteins Bax, Bcl-2, Caspase-3, and

Cleaved Caspase-3. Data are presented as mean ± SD; n = 5. *P < 0.05; **P < 0.01; ***P < 0.001 vs DMSO or control group.

Abbreviations: DMSO = dimethyl sulfoxide; SD = standard deviation.

Indirubin induces ALL cell cycle arrest in the G2/M phase

To clarify the impact of indirubin on cell cycle dynamics in ALL cells, flow cytometric analysis was performed. The results indicated a progressive accumulation of cells in the G2/M phase as indirubin concentration increased, suggesting a clear blockade at this checkpoint **(Figures 8a and 8b)**. Consistent with these findings, Western blot analysis showed reduced CDK1 and Cyclin B1 protein levels following indirubin treatment **(Figure 8c)**. These data indicate that indirubin inhibits ALL cell proliferation by interfering with the G2/M transition by suppressing CDK1 and Cyclin B1.

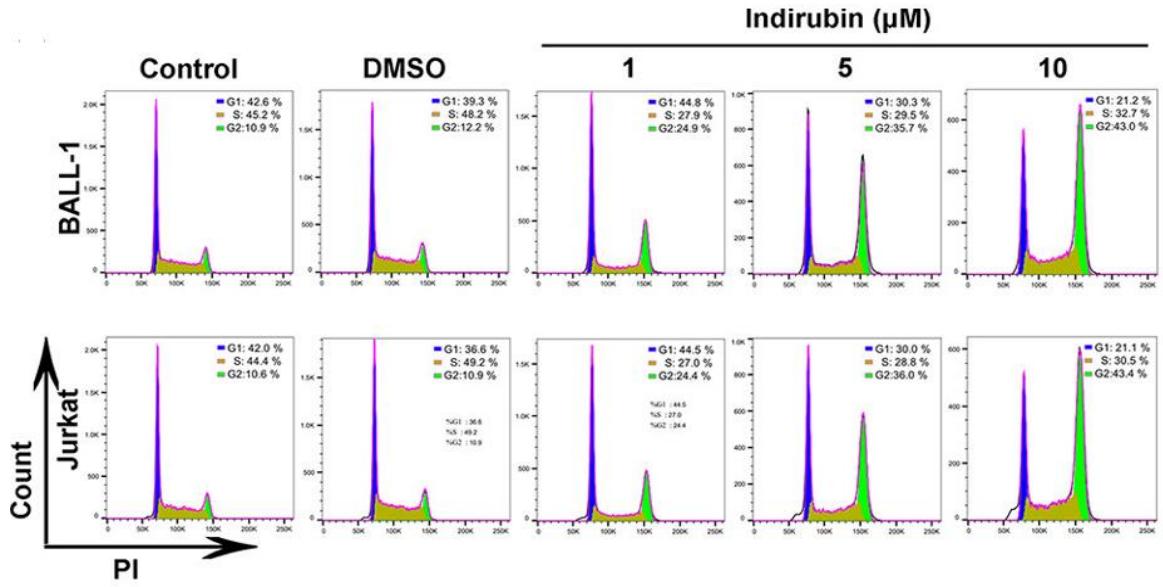

a)

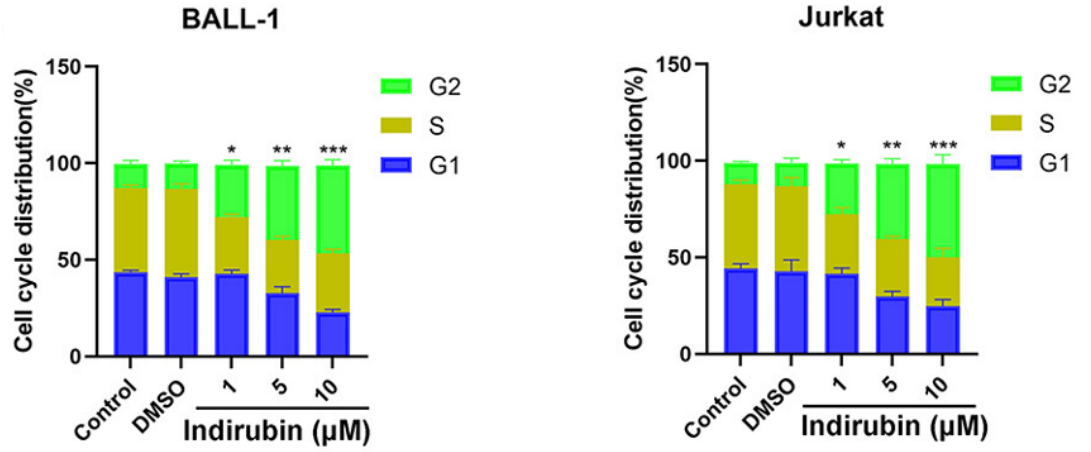

b)

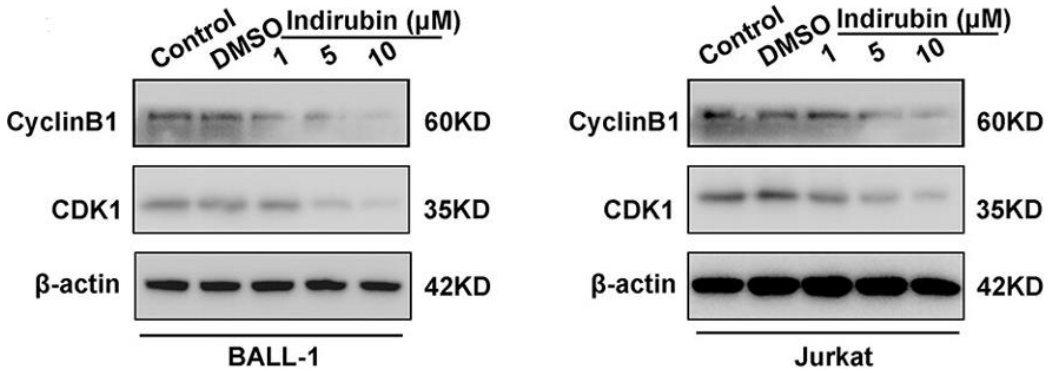

c)

Figure 8. Effect of indirubin on the cell cycle of ALL cells: (a and b) Flow cytometric analysis of cell cycle distribution, and (c) Expression of CDK1 and Cyclin B1 proteins related to cell cycle regulation. Data are presented as mean ± SD; n = 5. *P < 0.05; **P < 0.01; ***P < 0.001 vs DMSO or Control group. Abbreviations: DMSO = dimethyl sulfoxide; SD = standard deviation.

In vivo experimental verification of the action of indirubin on ALL cells

The anti-leukemic effect of indirubin was further validated in an in vivo xenograft model **(Figure 9a)**. Tumor growth in untreated nude mice showed continuous progression over time, whereas animals receiving indirubin exhibited markedly reduced tumor volume and weight compared with controls **(Figures 9b–9d)**. Throughout the experiment, no significant difference in body weight was observed between the two groups **(Figure 9e)**, suggesting minimal systemic toxicity.

Additionally, mononuclear cells isolated from bone marrow samples of six ALL patients were treated with 10 μM indirubin for 48 hours, resulting in a notable increase in apoptotic cells. These findings further confirm the tumor-inhibitory potential of indirubin (Figure 9F).

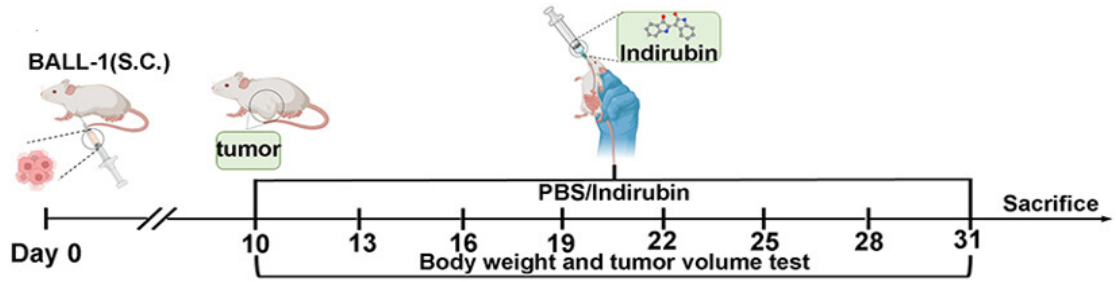

a)

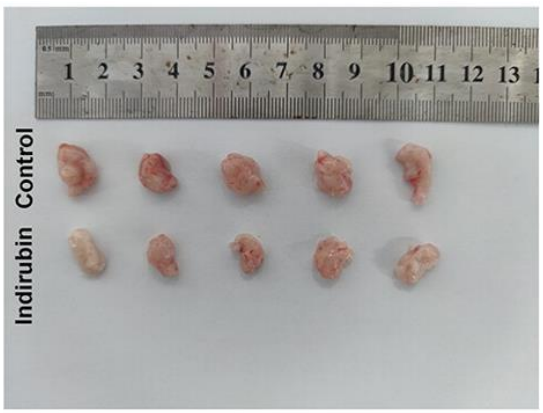

b)

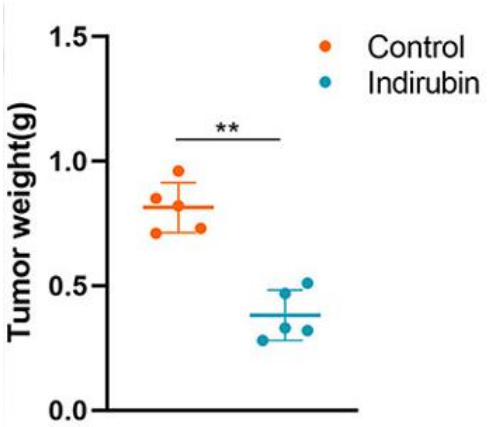

c)

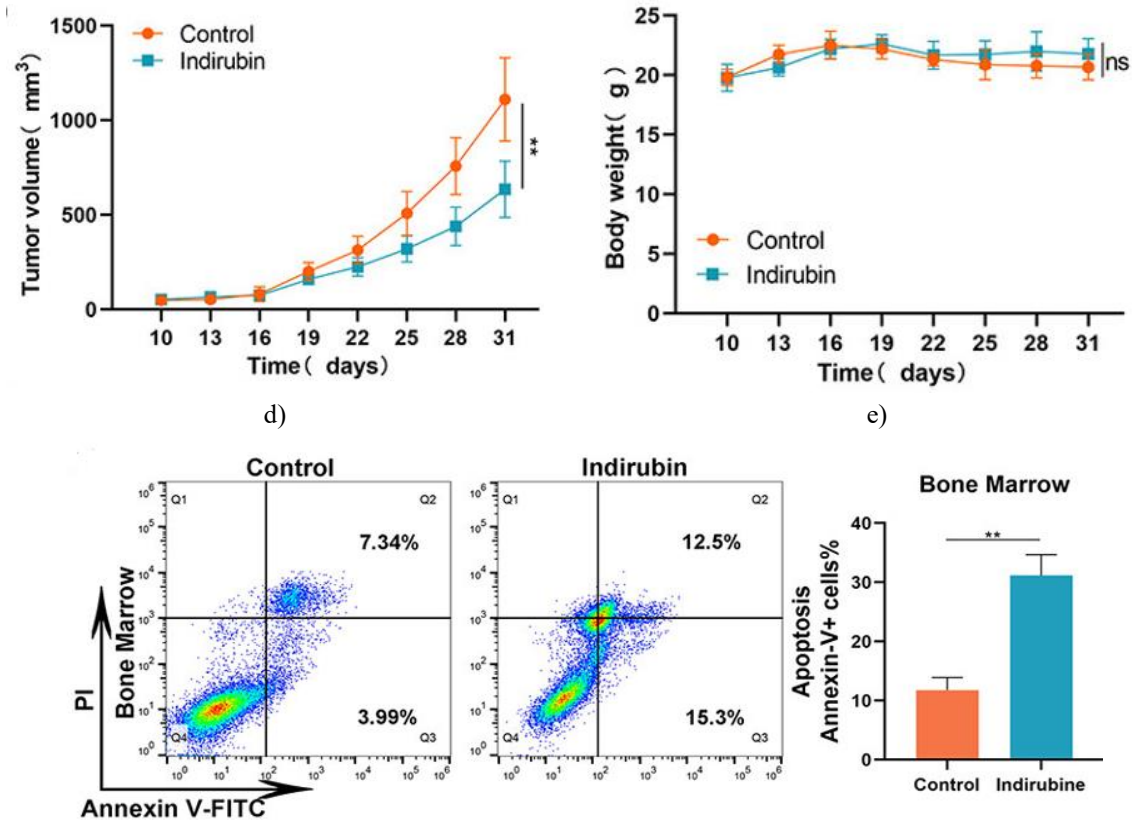

Figure 9. In vivo experimental verification of the action of indirubin on ALL cells: (a) Schematic representation of animal experimental design, (b) Xenograft tumor formation in nude mice (n = 5), (c) Tumor weight after 3 weeks of treatment, (d) Tumor volume changes over time, (e) Body weight monitoring during the experiment, and (f) Apoptosis of bone marrow mononuclear cells from ALL patients after treatment (n = 6). Data are presented as mean ± SD. **P < 0.01 vs Control group. Abbreviations: SD = standard deviation; ns = no significance.

Indirubin inhibits activation of the PI3K/Akt/mTOR signaling pathway

To elucidate the molecular mechanism underlying indirubin's anti-ALL activity, the PI3K-AKT signaling pathway was selected for validation based on GO and KEGG enrichment results and molecular docking analysis. Western blotting was performed to assess levels of PI3K/p-PI3K, AKT/p-AKT, and mTOR/p-mTOR proteins. The results showed that indirubin reduced phosphorylation of PI3K, AKT, and mTOR in a dose-dependent manner in ALL cells **(Figure 10).**

To further confirm pathway involvement, the PI3K/AKT agonist IGF-1 was introduced. IGF-1 treatment attenuated the effects of indirubin on apoptosis-related protein expression and restored indirubin-suppressed proliferative activity. Moreover, IGF-1 partially reversed the regulatory effects of indirubin on cell cycle-related proteins and PI3K/AKT/mTOR signaling components. Overall, these results indicate that the PI3K/AKT/mTOR pathway is a critical mediator of indirubin's anti-ALL effects.

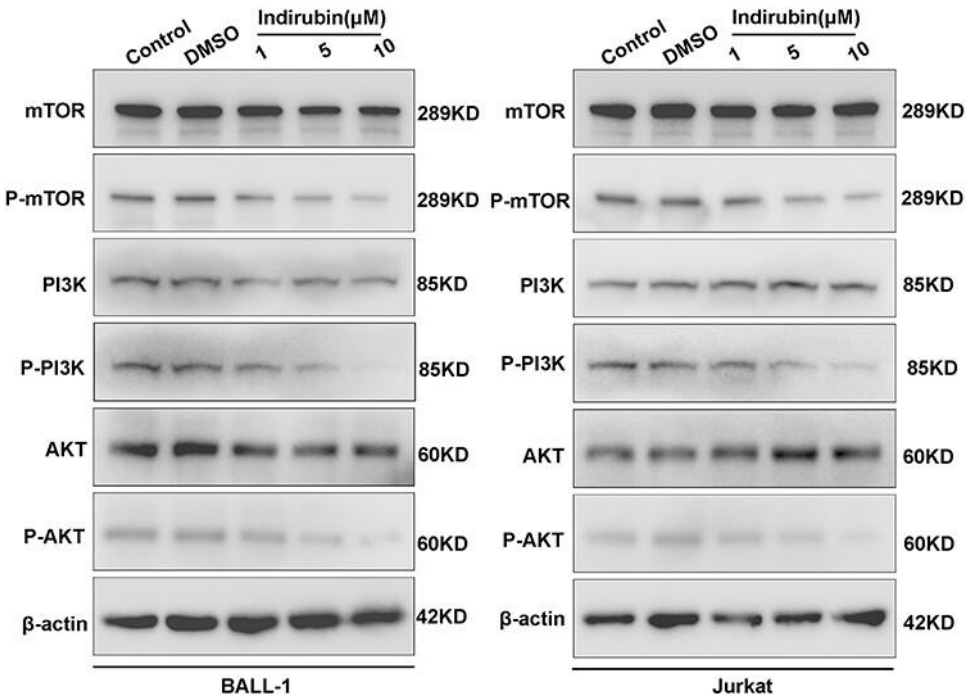

Figure 10. Western blot analysis of PI3K/AKT pathway proteins (PI3K/p-PI3K, AKT/p-AKT, mTOR/p-mTOR).

Acute lymphoblastic leukemia (ALL) is one of the most frequently occurring hematological malignancies. Although chemotherapy remains a standard treatment, patients often suffer from relapse and significant adverse effects, underscoring the urgent requirement for more effective and less toxic therapeutic options [16]. Indirubin, a bioactive compound isolated from *Indigofera tinctoria* L. and traditionally used in the treatment of chronic granulocytic leukemia, exhibits multiple pharmacological properties, including antitumor, anti-inflammatory, and neuroprotective effects, and inhibits various kinases [17]. In this context, network pharmacology has emerged as an important approach in modern drug discovery. Accordingly, the present study explored the anti-ALL mechanisms of indirubin through an integrated strategy combining network pharmacology, molecular docking, and experimental validation.

In the current analysis, 170 shared targets between ALL and indirubin were identified across multiple databases, and a corresponding protein–protein interaction (PPI) network was constructed. Using the CytoHubba algorithm, eight key hub genes were screened, including mTOR, CASP3, AKT1, matrix metalloproteinase 9 (MMP9), albumin (ALB), heat shock protein 90 alpha family class A member 1 (HSP90AA1), estrogen receptor 1 (ESR1), and prostaglandin-endoperoxide synthase 2 (PTGS2). These genes are closely involved in regulating apoptosis, cell proliferation, intracellular signaling, and cell cycle progression.

AKT1 is a central signaling kinase that governs both survival and proliferative pathways in cells. In leukemia, AKT1 phosphorylation promotes malignant cell growth and suppresses apoptosis [18]. In this study, indirubin treatment was found to markedly reduce phosphorylated AKT1 expression. ALB, the most abundant plasma protein, functions as a multifunctional carrier with enzymatic and binding activities; clinical evidence indicates that serum ALB levels are associated with prognosis and treatment response in leukemia patients [19]. HSP90AA1, a molecular chaperone linked to oncogenic processes, stabilizes tumor-associated proteins and enables cancer cells to withstand stress conditions, with elevated expression correlating with poor leukemia prognosis [20, 21]. Caspase-3 is a key executor of apoptosis, and its cleaved form directly mediates programmed cell death; in ALL, activated caspase-3 levels are also linked to clinical outcomes [22, 23]. Our results demonstrated that indirubin significantly enhanced cleaved caspase-3 expression.

ESR1 is a ligand-activated transcription factor responsive to estrogen, regulating gene transcription and DNA binding activity, and may exert effects through pathways such as PI3K/AKT and MAPK, making it a potential therapeutic target in leukemia [24]. MMP9 is a critical mediator of tumor invasion and metastatic behavior. Altered MMP9 expression has been observed in ALL bone marrow, and leukemia cells may stimulate its production via secreted factors, thereby enhancing invasiveness [25, 26]. PTGS2 is strongly associated with tumor

development and ALL progression; its upregulation has been reported in ALL, where it may influence disease behavior and represents a potential therapeutic target [27]. mTOR is a central regulator of cellular signaling networks controlling mRNA translation, cell cycle progression, transcriptional regulation, apoptosis, and metabolic activity. Clinical and experimental evidence indicate that elevated mTOR activity is associated with an unfavorable prognosis in ALL [28–30]. Collectively, these hub genes are critically involved in the initiation, progression, and clinical outcome of ALL.

Furthermore, the expression patterns of these key genes were examined using publicly available databases. Molecular docking results further confirmed that indirubin exhibits strong binding affinity for these targets, suggesting that its anti-ALL effects may be mediated by direct interactions with these core regulatory genes and subsequent inhibition of disease progression.

To gain a system-level understanding of how indirubin may act in ALL, GO, and KEGG enrichment analyses were carried out on the 170 intersecting targets. GO functional profiling indicated that indirubin-related genes were mainly involved in processes such as cellular adaptation to chemical stress, regulation of kinase activation, and oxidative stress response, as well as other interconnected biological activities. These patterns imply that indirubin likely influences ALL through coordinated modulation of multiple biological processes rather than acting on a single pathway.

KEGG pathway analysis further refined these findings, showing that the most significantly enriched signaling pathways included PI3K-AKT, RAS, and FoxO, all of which are strongly implicated in leukemic transformation and disease progression. Given the enrichment strength and target distribution, the PI3K-AKT pathway was selected as the primary focus, as it likely represents a central axis of indirubin-mediated effects in ALL. This pathway is a key intracellular signaling system governing oxidative balance, inflammatory regulation, cell proliferation, growth, and survival [31–33]. It can be activated by diverse extracellular inputs, including receptor tyrosine kinases, integrins, antigen receptors on B and T cells, and G protein-coupled receptors [34, 35]. In hematopoietic biology, PI3K-AKT signaling is essential for both normal blood cell development and malignant transformation. Importantly, aberrant activation of this pathway is detected in approximately 88% of ALL cases and is closely linked to chemoresistance and unfavorable clinical outcomes [36–38]. To support this relevance, prior studies have shown that CASZ1 promotes T-cell ALL progression by activating PI3K-AKT-mTOR signaling [39]. Similarly, *Brucea javanica* seed oil has been reported to induce apoptosis in Jurkat leukemia cells by inhibiting the PI3K/Akt signaling pathway [40]. Collectively, these findings highlight PI3K-AKT signaling as a key therapeutic vulnerability in ALL. Consistently, the core targets identified in this study were predominantly enriched in this pathway.

Experimental validation was then performed to confirm the computational predictions. In vitro assays demonstrated that indirubin significantly reduced ALL cell proliferation, promoted programmed cell death, and caused accumulation of cells in the G2/M phase. In vivo studies further confirmed that indirubin effectively suppressed leukemia progression. Examination of key proteins in the PI3K-AKT cascade showed that indirubin alters their expression profiles, supporting the pathway's involvement. Overall, these results suggest that indirubin exerts anti-leukemic activity largely by modulating PI3K-AKT signaling. However, certain limitations should be acknowledged. First, the study did not include comparisons with other standard anti-ALL drugs or evaluate possible synergistic combination therapies. Second, although multiple molecular targets and pathways were identified, the regulatory network underlying indirubin activity is complex and likely extends beyond the pathways analyzed, warranting further mechanistic investigation.

Conclusion

This work systematically examined the anti-ALL potential of indirubin from an integrated mechanistic perspective. By combining network pharmacology analysis, molecular docking simulations, and experimental validation, the study demonstrated that indirubin acts through multiple molecular targets and signaling pathways, with PI3K-AKT signaling playing a central role (Figure 11). These findings provide supportive evidence for considering indirubin as a promising candidate for ALL therapy.

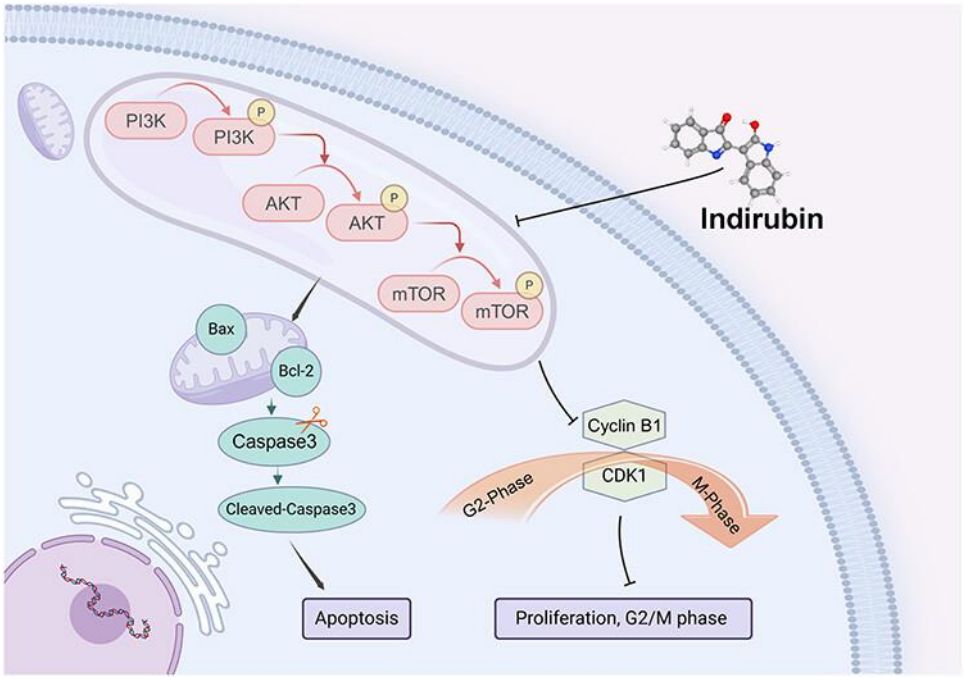

Figure 11. Proposed mechanistic model of indirubin action in ALL. Image generated using BioRender.com with permission.

Acknowledgments: We express our gratitude to the Children's Blood Centre at Guizhou Medical University Hospital for kindly providing the bone marrow specimen.

Conflict of Interest: None

Financial Support: This study was supported by the National Natural Science Foundation of China (No. 32270848, U23A20498) and the Guizhou Province Science and Technology Project (LC[2022]001, Qian Ke He[2019]5406).

Ethics Statement: Animal experiments in the study protocol were reviewed and approved by the Animal Ethics Committee of Guizhou Medical University (No. 2400569). The use of ALL bone marrow samples in this study was approved by the Guizhou Medical University Human Experimentation Ethics Committee. This study was conducted in accordance with the principles of the Declaration of Helsinki. Written informed consent was obtained from all patients before sample collection.

References

1. Gower M, Tikhonova AN. Under the surface: scratching the acute lymphoblastic leukemia niche. Haematologica. 2023;108(5):1210-2.
2. Pagliaro L, Chen SJ, Herranz D, Ballerini P, Béné MC, Biondi A, et al. Acute lymphoblastic leukaemia. Nat Rev Dis Primers. 2024;10(1):41.
3. Dong Y, Shi O, Zeng Q, Lu X, Wang W, Li Y, et al. Leukemia incidence trends at the global, regional, and national level between 1990 and 2017. Exp Hematol Oncol. 2020;9(1):14.
4. Siegel RL, Giaquinto AN, Jemal A. Cancer statistics, 2024. CA Cancer J Clin. 2024;74(1):12-49.
5. Hunger SP, Raetz EA. How I treat relapsed acute lymphoblastic leukemia in the pediatric population. Blood. 2020;136(16):1803-12.
6. Zhang X, Qiu H, Li C, Cai P, Qi F. The positive role of traditional Chinese medicine as an adjunctive therapy for cancer. Biosci Trends. 2021;15(5):283-98.
7. Yang L, Li X, Huang W, Rao X, Lai Y. Pharmacological properties of indirubin and its derivatives. Biomed Pharmacother. 2022;151:113112.

8. Wang H, Wang Z, Wei C, Wang L, Chen Z, Zhang Y, et al. Anticancer potential of indirubins in medicinal chemistry: biological activity, structural modification, and structure-activity relationship. Eur J Med Chem. 2021;223:113652.
9. Chen L, Wang J, Wu J, Zheng Q, Hu J. Indirubin suppresses ovarian cancer cell viabilities through the STAT3 signaling pathway. Drug Des Devel Ther. 2018;12:3335-42.
10. Zhu JM, Chen C, Kong M, Li X, Zhang Y, Wang H, et al. Discovery and optimization of indirubin derivatives as novel ferroptosis inducers for the treatment of colon cancer. Eur J Med Chem. 2023;261:115829.
11. Mohan L, Raghav D, Ashraf SM, Sebastian J, Rathinasamy K. Indirubin, a bis-indole alkaloid binds to tubulin and exhibits anti-mitotic activity against HeLa cells in synergism with vinblastine. Biomed Pharmacother. 2018;105:506-17.
12. Zhao L, Zhang H, Li N, Sun X, Chen X, Wang Y, et al. Network pharmacology, a promising approach to reveal the pharmacology mechanism of Chinese medicine formula. J Ethnopharmacol. 2023;309:116306.
13. Zhang P, Zhang D, Zhou W, Chen Y, Liu X, Li H, et al. Network pharmacology: towards the artificial intelligence-based precision traditional Chinese medicine. Brief Bioinform. 2024;25(1):bbad518.
14. Agu PC, Afiukwa CA, Orji OU, Eze PM, Ogbu CP, Ugwu OP, et al. Molecular docking as a tool for the discovery of molecular targets of nutraceuticals in diseases management. Sci Rep. 2023;13(1):13398.
15. Chen S, Li B, Chen L, Jiang H. Uncovering the mechanism of resveratrol in the treatment of diabetic kidney disease based on network pharmacology, molecular docking, and experimental validation. J Transl Med. 2023;21(1):380.
16. Inaba H, Mullighan CG. Pediatric acute lymphoblastic leukemia. Haematologica. 2020;105(11):2524-39.
17. Lee JH, Shin JE, Kim W, Lee S, Park J, Kim H, et al. Discovery of indirubin-3'-aminooxy-acetamide derivatives as potent and selective FLT3/D835Y mutant kinase inhibitors for acute myeloid leukemia. Eur J Med Chem. 2022;237:114356.
18. Astolfi A, Milano F, Palazzotti D, Piergentili A, Del Bello F, Camaioni E, et al. From serendipity to rational identification of the 5,6,7,8-tetrahydrobenzo[4,5]thieno[2,3-d]pyrimidin-4(3H)-one core as a new chemotype of AKT1 inhibitors for acute myeloid leukemia. Pharmaceutics. 2022;14(11):2295.
19. Zhang Y, Chen Q, Lu C, Yu L. Prognostic role of controlling nutritional status score in hematological malignancies. Hematology. 2022;27(1):653-8.
20. Wang Z, Fan L, Xu H, Wang Y, Zhang X, Liu J, et al. HSP90AA1 is an unfavorable prognostic factor for hepatocellular carcinoma and contributes to tumorigenesis and chemotherapy resistance. Transl Oncol. 2024;50:102148.
21. Wu YW, Chao MW, Tu HJ, Lin KT, Chen YL, Tseng LM, et al. A novel dual HDAC and HSP90 inhibitor, MPT0G449, downregulates oncogenic pathways in human acute leukemia in vitro and in vivo. Oncogenesis. 2021;10(5):39.
22. Montiel-Cervantes LA, Reyes-Maldonado E, Garcia-Chavez J, Rosas-Cabral A, Cervera-Ceballos E, Herrera-Garcia A, et al. Prognostic value of CD95, active caspase-3, and Bcl-2 expression in adult patients with de novo acute lymphoblastic leukemia. Arch Med Res. 2018;49(1):44-50.
23. Jiang M, Qi L, Li L, Li Y. The caspase-3/GSDME signal pathway as a switch between apoptosis and pyroptosis in cancer. Cell Death Discov. 2020;6(1):112.
24. Liu Q, Liu Y, Li X, Wang H, Zhang Y, Chen Z, et al. Perfluoroalkyl substances promote breast cancer progression via ERα- and GPER-mediated PI3K/Akt and MAPK/Erk signaling pathways. Ecotoxicol Environ Saf. 2023;258:114980.
25. Verma D, Zanetti C, Godavarthy PS, Kumar R, Minciacchi VR, Pfeiffer J, et al. Bone marrow niche-derived extracellular matrix-degrading enzymes influence the progression of B-cell acute lymphoblastic leukemia. Leukemia. 2020;34(6):1540-52.
26. Augoff K, Hryniewicz-Jankowska A, Tabola R, Stach K. MMP9: a tough target for targeted therapy for cancer. Cancers (Basel). 2022;14(7):1847.
27. Cruz-Miranda GM, Olarte-Carrillo I, Bárcenas-López DA, Hernández-Ramírez VI, Vázquez-Medina JP, Saldaña-Alvarez Y, et al. Transcriptome analysis in Mexican adults with acute lymphoblastic leukemia. Int J Mol Sci. 2024;25(3):1750.
28. Simioni C, Martelli AM, Zauli G, Melloni E, Neri LM. Targeting mTOR in acute lymphoblastic leukemia. Cells. 2019;8(2):190.

29. Ge Z, Song C, Ding Y, Tan Y, Fu Y, Li H, et al. Dual targeting of MTOR as a novel therapeutic approach for high-risk B-cell acute lymphoblastic leukemia. Leukemia. 2021;35(5):1267-78.
30. Glaviano A, Foo ASC, Lam HY, Yap KC, Alharthi H, Loh JJT, et al. PI3K/AKT/mTOR signaling transduction pathway and targeted therapies in cancer. Mol Cancer. 2023;22(1):138.
31. Yu L, Wei J, Liu P. Attacking the PI3K/Akt/mTOR signaling pathway for targeted therapeutic treatment in human cancer. Semin Cancer Biol. 2022;85:69-94.
32. He Y, Sun MM, Zhang GG, Yang J, Chen KS, Xu WW, et al. Targeting PI3K/Akt signal transduction for cancer therapy. Signal Transduct Target Ther. 2021;6(1):425.
33. Huang J, Chen L, Wu J, Ren C, Chen Y, Xu Y, et al. Targeting the PI3K/AKT/mTOR signaling pathway in the treatment of human diseases: current status, trends, and solutions. J Med Chem. 2022;65(24):16033-61.
34. Li Q, Li Z, Luo T, Shi H. Targeting the PI3K/AKT/mTOR and RAF/MEK/ERK pathways for cancer therapy. Mol Biomed. 2022;3(1):47.
35. Liu R, Chen Y, Liu G, Li C, Song Y, Cao Z, et al. PI3K/AKT pathway as a key link modulates the multi-drug resistance of cancers. Cell Death Dis. 2020;11(9):797.
36. Nepstad I, Hatfield KJ, Grønningsæter IS, Reikvam H. The PI3K-Akt-mTOR signaling pathway in human acute myeloid leukemia (AML) cells. Int J Mol Sci. 2020;21(8):2907.
37. Wiese W, Barczuk J, Racinska O, Winiarska M, Graczyk-Jarzynka A, Krawczyk M, et al. PI3K/Akt/mTOR signaling pathway in blood malignancies—new therapeutic possibilities. Cancers (Basel). 2023;15(21):5297.
38. Sanchez VE, Nichols C, Kim HN, Gang EJ, Kim YM. Targeting PI3K signaling in acute lymphoblastic leukemia. Int J Mol Sci. 2019;20(2):412.
39. Cardoso BA, Duque M, Gírio A, Henriques A, Martins LR, Carvalho T, et al. CASZ1 upregulates PI3K-AKT-mTOR signaling and promotes T-cell acute lymphoblastic leukemia. Haematologica. 2024;109(6):1713-25.
40. Zhang H, Yin SL, Wang LH, Liu YQ, Chen JX, Li W, et al. Seed oil of Brucea javanica induces apoptosis through the PI3K/Akt signaling pathway in acute lymphocytic leukemia Jurkat cells. Chin J Nat Med. 2021;19(8):608-20.